DOI: 10.37190/ABB-02392-2024-03

Virtual modelling the impact of torsional loading on osteoporotic vertebrae buckling

Olga Chabarova[1], Jelena Selivonec[1]*

[1]Department of Applied Mechanics, Vilnius Gediminas Technical University, Vilnius, Lithuania
*Corresponding author: Jelena Selivonec; Vilnius Gediminas Technical University, Saulėtekio al. 11, Vilnius 10223, Lithuania, e-mail: jelena.selivonec@vilniustech.lt

Submitted: 31st January 2024
Accepted: 15th April 2024

Abstract

Purpose

This study aimed to evaluate the biomechanical response or load transfer on the osteoporotic L1 vertebra under torsional loading.

Methods

To achieve this goal, a numerical model of osteoporotic vertebra in various trabecular bone degenerations was developed and tested. The mechanical behavior of the model was represented taking into account the anisotropic properties of the cancellous bone, which provided a more realistic mechanical picture of the biological subsystem. To ensure the reliability of osteoporotic degradation, the thinning of cortical bone and the appearance of gaps between trabecular bone and cortical bone were also taken into account when creating the models.

Results

Finite element (FE) analysis showed that the deformations of cortical bone thinning and detachment of the cortical bone from the trabecular tissue lead to local instability of the vertebrae. As a result, the cortical bone of a vertebra loses its load-bearing capacity, even if the strength limit is not reached.

Conclusions

The results obtained allow us to state that taking into account the thinning of the trabeculae, which creates voids, is extremely important for load-bearing capacity of osteoporotic vertebrae. However, a limitation of this study is the lack of experimental data to ensure consistency with the computer simulation results.

Keywords: Osteoporosis; Lumbar spine; Vertebra; FEM; Instability.

1.Introduction

The vertebrae of the spine bear most of the vertical load placed on the body. The most loaded part of the spine is the lumbar spine, i.e., the spine fragment composed of L1–L5 vertebrae, which has to bear the essential part of the human-induced load compared to the other spinal parts [8], [13], [33].

From a medical point of view, harmful spinal pathology is one of the main health problems. Osteoporosis is one of the causes of the spinal pathology that spreads among people more and more widely.

Osteoporosis is a disease characterized by decreased bone density and micro, sometimes macro damages of the bone tissue, resulting in increased brittleness of bones. Although osteoporosis affects the entire skeleton of the body, most osteoporotic fractures are associated with the spinal vertebrae. Specifically, compression-induced fracture of the spine usually occurs at the first vertebra of the lumbar spine (L1) [14].

Due to the above – listed reasons, the excessive deformation of the vertebrae is a very real problem in today's medicine. Prevailing existing methodologies for the diagnostic and prognosis of the pathologies and the excessive deformations of the human vertebrae are based on the analysis of computer tomography images [6].

In medicine, the tool FRAX (Fracture Risk Algorithm) is used to predict the risk of a vertebral fracture. This tool is based only on human physiological parameters such as age, sex, height, weight, etc., and physical parameters such as bone mineral density (BMD) [35]. These diagnostic techniques do not take into account all factors of vertebrae degeneration to predict the risk of vertebral fracture. Despite significant advances in the small-scale evaluation of the mechanical properties of lumbar bone tissue [23], [27], the understanding of osteoporotic changes and the contribution to functionality is not satisfactory. Therefore, the numerical analysis of the human vertebrae by taking into account the reasons affecting its deformations can be used to select the most effective treatment method [26].

In the work [24] healthy and osteoporotic vertebrae L1 were analysed to determine their biomechanical response. FE analysis shows that one of the most important factors in osteoporosis is the tendency to increase tension in the cancellous bone of the vertebra. Studies analysing spine under torsion [10], [15] suggested possible vertebral fractures using the mechanical criteria of plasticity and fracture, but did not take into account the relationship between vertebral deformity and loss of load-bearing capacity.

In the works [3]-[5] there have already been studies of models of lumbar spine that considered osteoporotic changes in the trabecular bone of the vertebrae as a decrease in BMD. The above-mentioned studies did not consider the possibility of voids appearing in the trabecular bone and their impact on the local stability of an individual osteoporotic vertebra under torsional loading. The aim of this study is to advance knowledge of the macroscopic deformation behaviour of degenerated osteoporotic lumbar vertebrae by recovering the effects of nonlinear geometric deformations that cause cortical shell instability.

Computational simulation methods can help analyse in more detail the degradation bone tissue and determine its effect on vertebral deformation, which cannot be tested with experimental methods [36]. Computational simulation can save time and reduce investigation

costs. In addition to saving time, computer modelling eliminates the need for costly and time-consuming laboratory testing.

2. Materials and methods

2.1. Motivation

The mechanical state characteristics of the lumbar vertebrae in conditions of osteoporotic bone tissue degeneration are considered using structural analysis with the finite element method. The decision to develop this survey can be motivated by the following arguments.

- New results can be obtained by exploring the already known continuous two-phase model. From a mechanical point of view, the essential properties of the vertebral body can be obtained by considering it on a macroscopic scale. The trabecular volume is viewed as a three-dimensional continuum, while the dense cortical layer is viewed as a thin shell. This two-phase model - cortical shell and trabecular volume - is mechanistically justified and is often examined in numerical modelling [2], [18]-[19], [29], [39]. The above partitioning problem is somewhat hypothetical. The classification of a specific subvolume into the cortical or trabecular phase can be based on CT imaging based on the value of the porosity (density) [12]. It has been observed that osteoporotic degeneration causes gross changes as a result of bone loss, but the mechanism of degradation is not trivial. Most of the absolute bone loss due to osteoporosis occurs in the interlayer of bone between the two phases. Cortical bone through the so-called intracortical bone layer, where pores exist, the transition zone is enlarged, is formed as shown in Figure 1 b, c [38]. This means a reduction in the thickness of the cortical layer. Furthermore, the concentrated reduction in degraded thickness in the presence of pores can be considered as an imperfection of potential instability factors.
- New properties could be implemented by analysing virtual models, applying large displacement and deformation calculation methods. Finding deformation instability requires more enhanced nonlinear analysis. Instability is a process during which a given structure cannot sustain load in its initial form [21]. This is a buckling-type failure mechanism relevant to out-of-plane deformation of thin-walled structures, which are very sensitive to small imperfections. It is obvious that a vertebra looking like a stiffened cylindrical shell structure is potentially risky to instability. Therefore, the load-bearing capacity of the spine may be lost, not only by fracture but also by the

occurrence of instability. Failure risk increases during osteoporotic degeneration because of the thinning of the cortical shell and the presence of imperfections.

- A new quality could be achieved by the same technique — the FEM. In this study, the numerical finite element analysis is utilised to demonstrate the potential of this tool in the evaluation of the risk of osteoporotic degradation. The particular advantages of the finite element analysis will be explored by developing a universal finite element model able to solve various mechanical problems using the same geometry. On the other hand, the unified model integrates the external shell and the internal 3D solid while regarding different bonding between them.

2.2. Development of model geometry

A three-dimensional virtual model of the vertebra L1 was developed in several steps. Firstly, a CT scan was performed on a 48-year-old man. The resulting images were then processed using the free open source software 3D Slicer [40] and refined using MeshLab [42]. Using the semiautomatic tool in the 3D Slicer software, a region of interest was defined around L1, and its 3D volumetric image was segmented. A minimum threshold mode was set between 80 and 100 to separate soft tissues from the vertebral body. The endplates, posterior bone elements and articular facets were not included in image analyses and were manually removed.

The MeshLab output of the 3D volumetric image of L1 STL file was exported to the SolidWorks software environment [43], where final mesh rendering was performed and the surfaces were converted into a solid model of the lumbar vertebral body. Posterior bony elements are added manually to reflect the stiffening of the vertebra's back part. Two bony endplates are also added to reflect boundary conditions with the neighbouring trabecular bone. The final numerical model is shown in Figure 1 a.

The internal geometry of the vertebral body is constructed to reflect both the healthy state and osteoporotic degeneration. The degree of degeneration is characterised by the reduction of the cortical bone thickness layer, t_{cor}, which is dependent on the severity of osteoporosis. The classification of a specific subvolume into the cortical or trabecular phase was performed based on the values of porosity (density) [9].

The occurrence of voids between the two phases, cortical and trabecular bone, is introduced as unbonded contact using the contact tool of the ANSYS software [41].

Offsets of specific values are added to the top endplate to determine the bifurcation point and critical force. The lower endplate of the vertebra is rigidly fixed.

2.3. Mechanical properties

The cortical phase is modelled as an isotropic elasto-plastic continuum. The trabecular phase is modelled as an elastic orthotropic continuum. Therefore, the transverse modulus of elasticity is assumed to be a fraction of the longitudinal modulus. The mechanical properties of trabecular bone were calculated based on bone mineral density obtained from CT images, as shown in [3]. It is assumed that the distribution of material mechanical properties is uniform within each subvolume. The spinous process, superior articular process, transverse process and vertebral endplates are described as linear elastic isotropic material. The physical properties of the different components of the vertebral body are summarised in Table 1 Different properties are attributed to different grades. The basic characteristics of the grades are given in Table 2.

Table 1: Vertebra's material properties of the components.

System	Young modulus [MPa]	Poisson ratio
Cortical bone [9], [17], [30]	E_{cor} = 8000	v_{cor} = 0.3
Cancellous bone (healthy / osteoporotic) [3]	$E_{can,xx}$ = 130 / 13	$v_{can,xy}$ = 0.3
	$E_{can,yy}$ = 130 / 13	$v_{can,yz}$ = 0.2
	$E_{can,zz}$ = 723 / 72.3	$v_{can,xz}$ = 0.2
	$G_{can,xy}$ = 27.8 / 5	
	$G_{can,yz}$ = 48.2 / 8.7	
	$G_{can,xz}$ = 48.2 / 8.7	
Vertebral bony endplate [16], [28]	E_{pl} = 25	v_{pl} = 0.4
Posterior Bone [11], [16], [37]	E_{pb} = 3500	v_{pb} = 0.25

Table 2: Characterization of age-related degeneration.

Grades of age-related degeneration	grade 1 (healthy)	grade 2 (osteoporotic)	grade 3 (osteoporotic)	grade 4 (osteoporotic)
Cancellous bone (density [kg/m^3]) [3]	300	100	100	100
Thickness of Cortical bone (t_{cor}) [mm]	0.5	0.4	0.2	0.2

Connection type between to phase	bonded	bonded	bonded	unbonded

2.4. Mathematical model

In this study, the mechanical state properties of lumbar vertebrae in osteoporotic bone tissue degeneration were analysed through finite element method structural analysis. The study explores the advantages of finite element analysis by developing a universal finite element model that can solve various mechanical problems using the same geometry. The unified model integrates the outer shell and the inner 3D solid, respecting the different constraints between them.

The stability problem is formulated as a geometrically nonlinear analysis problem. For a discrete structure, the problem is described by a system of nonlinear algebraic equations, as shown in equation:

$$\mathbf{K}_G\left(\mathbf{u}(t)\right)\mathbf{u}(t)=\mathbf{F}(t), \tag{1}$$

where **u** is the displacement vector describing the state of the structure; **F** – external load vector; $\mathbf{K}_G$ – stiffness matrix of the deformed structure; time *t* is a dimensionless quantity whose values vary between 0 and 1. This quantity is the deformation of the structure (load variation) indicator describing the course of the process.

When studying stability, a typical case of loss of stability can be distinguished. The most characteristic loss of stability is associated with the bifurcation point. The critical condition is characterized by the value of the critical force (bifurcation point) and the possible post-critical operation of the system with a lower critical force.

In this work, the structural stability indicators are related to the determination of these bifurcation points and the critical values of the forces and displacements occurring at these points.

Since the solution to the problem includes not only displacements but also stresses, the mathematical model (1) allows evaluating the strength criteria as well. To determine the stress and bone strength, the classic plasticity criterion at a continuous level is often applied. Therefore, the von Mises stress criterion is the most frequently used criterion [32] for the trabecular bone of the vertebrae.

The external axial load at time *t* is given as the vertical displacement $u_z(t_{max}) = u_{z,max}$ limited by maximal value $u_{z,max}$ = 1 mm, and the torque as the angle of rotation $\omega_z(t_{max}) = \omega_{z,max}$ limited by maximal value $\omega_{z,max} = 10^o$.

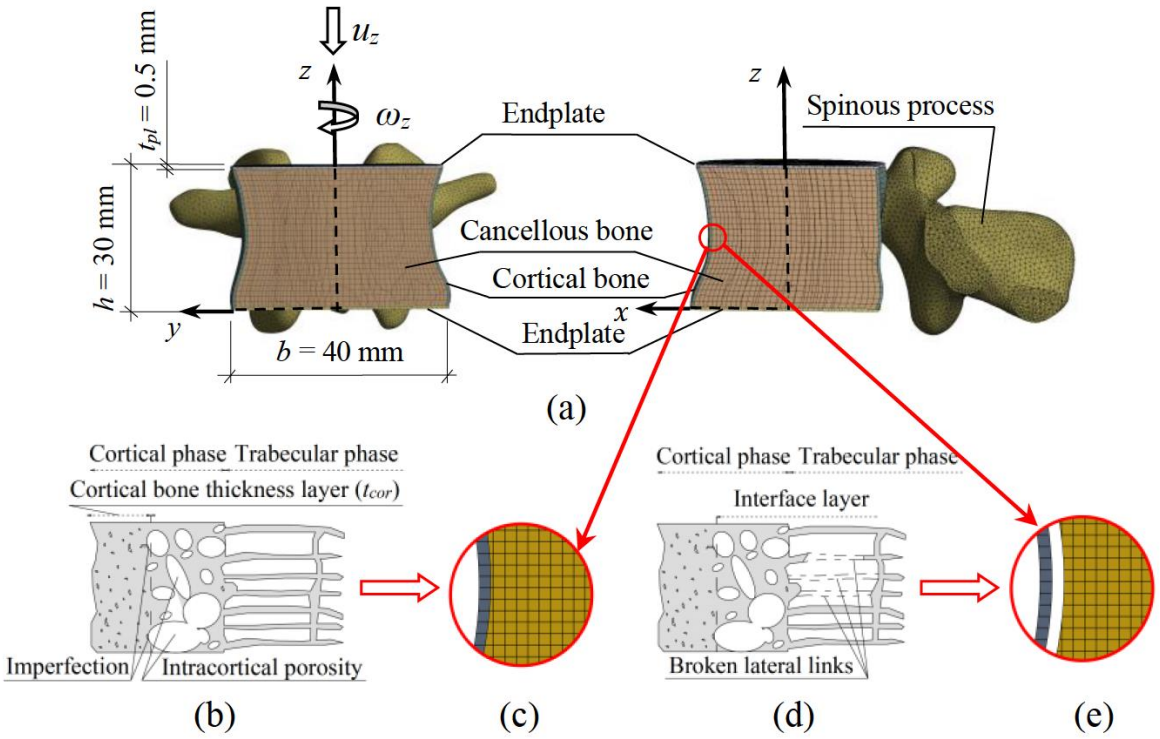

Figure 1: A view of the model: (a) L1 vertebra's cross-section FE model. (b), (d) The schematisations of the degenerative bone structure. (c) Bonded connection. (e) Unbonded connection with a gap.

To handle inequality constraints when solving contact problems, an extended Lagrangian approach is used. The displacements are specified to find the bifurcation point and trace the descending branch of the load during buckling of the load.

This reflects the two failure cases: loss of the load-bearing capacity defined by strength (plastic yielding) criteria and loss of stability (buckling) defined by deformation criteria. Buckling is traditionally considered as buckling of the cortical shell characterised by elastic instability due to the critical out-of-plane deformation of a structure reached under the action of an axial (in-plane) load. A critical state is characterised by the value of a critical load at a (bifurcation) point. In the presence of continuum regions, the critical instability may be characterised as the asymptotic limit state having unlimited deformation of the continuum part. For evaluation of the strength limit, the additional model for perfect plasticity is optionally switched.

The vertebral body of the anatomic shape shown in Figure 1a is considered as the solution domain described by finite elements. Shell and volumetric domains may be connected in a different manner. The discretization is performed by applying the pre-processor of the

ANSYS code [22]. Four different finite element models were created to describe the grade 1, grade 2, grade 3, and grade 4 samples mentioned above for modelling purposes.

The mesh convergence of one of the four FE models was tested. Three different mesh resolutions were created for this model. Mesh 1 uses minimum element sizes that correspond to the thickness of the cortical bone. Consequently, Mesh 1 had the largest number of elements and nodes among the three mesh resolutions. In the next mesh the size of the elements was doubled, in the last mesh – three times. The number of elements and nodes for each mesh resolution is shown in Table 3.

Table 3. Number of elements and nodes of different resolutions of the FE mesh.

System	Element number	Node number
Mesh 1	758 949	1 853 700
Mesh 2	147 210	335 656
Mesh 3	107 747	207 035

In this study, three mesh resolutions were tested at the same axial rotation. A mesh is considered convergent if the results obtained using two successive mesh resolutions differ by no more than 5% [1], [16]. The percentage differences in strain and von Mises stress between Mesh 1 and Mesh 2 and Mesh 1 and Mesh 3 are shown in Figure 2. The differences in von Mises stresses and strains between mesh 1 and mesh 2 were less than 5% in all fabrics of the model. Therefore, mesh 2 is considered to be convergent in stress and strain (Fig. 2). When studying the models, a mesh with element's side length of 1 mm was used.

Cortical bone was discretized from finite element shells. The BE grid contains 2976 shell elements with 3094 nodes. Each shell element has four nodes with six degrees of freedom at each node: linear displacements in the x, y and z directions and angular displacements about the x, y and z axes. Elements can be connected through nodes using both midline and outer nodes. These shell elements associated with larger deformation and bending are able to describe the instability of the structure.

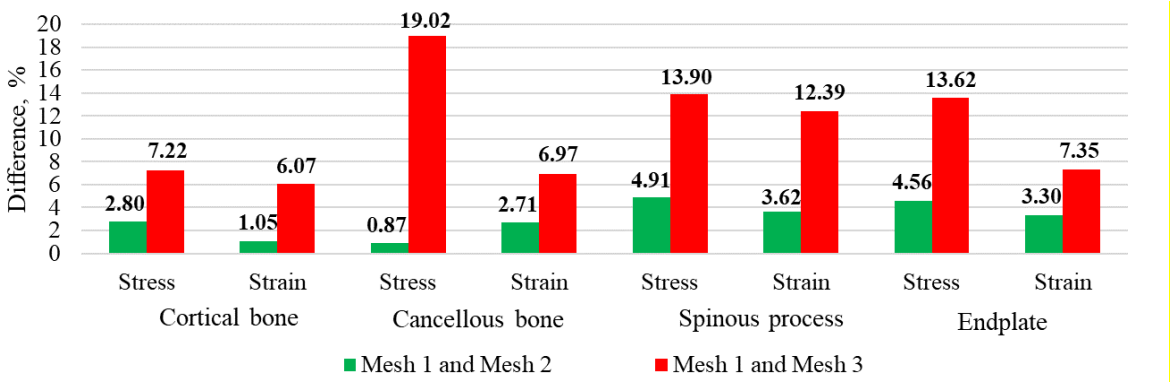

Figure 2: Percentage differences in von Mises stresses and strains in different tissues between Mesh 1 and Mesh 2 and between Mesh 1 and Mesh 3 in the axial rotation.

The trabecular bone, posterior bone, and endplate models of the vertebra were discretized from volumetric finite elements The model contains 144 234 volumetric elements with 332 562 nodes. The BE mesh model is shown in Figure 1a.

The trabecular bone, posterior bone and endplate models were discretized automatically from volumetric finite elements SOLID186. This type of solid is a 20 node higher order 3D solid that approximates a quadratic displacement. Elements may be in cube, prism and pyramid shapes. The element supports large strain, large deflection and plasticity.

3. Results

To evaluate the contribution of osteoporotic degradation, a series of numerical experiments using the above-discussed finite element model equation (1) were conducted.

For the analysis of the obtained results, point A of the cortical bone was selected, the position of which was closer to the expected zone of loss of local stability (Fig. 3, Fig. 4).

Essentially, the characterization of osteoporotic degradation is an illustration of displacements and stresses achieved under loading. The physical nature of different models is qualitatively illustrated by deformed shapes, and a colour plot of the displacement magnitude of the cortical shell is shown in Figure 3. The displacement values, defined in millimetres, are illustrated in a unified colour scale. The first three subfigures (a, b, c) illustrate bonded shell-solid contact, while the last subfigure (d) illustrates unbonded contact. The first column (a) shows the results obtained for a healthy vertebra with a large shell thickness of 0.5 mm. The second column (b) shows the results obtained for an osteoporotic vertebra with a decrease in the thickness of the shell to 0.4 mm, while the third and fourth columns (c, d) show results for the most degraded cortical shell. Characterising deformation shapes in a colour scale clearly illustrates the degree of degradation. Unbonded contact leads to the occurrence of two higher-order deformation modes. Near point B, an extremely large displacement can be observed (Fig. 3 d). An extremely large displacement occurs, exceeding 8 times the thickness of the cortical bone (Fig. 3d). This result indicates shell buckling.

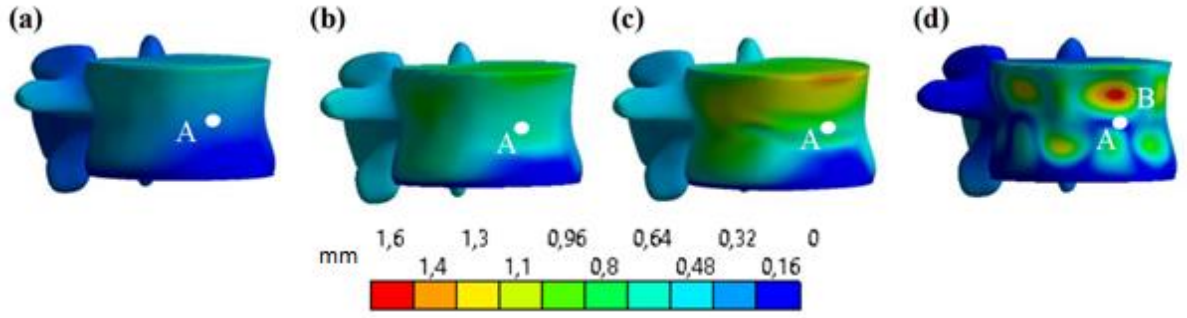

Figure 3: Effect of the deformed shape at the first bifurcation point. (a) Bonded trabecular bone, $t_{cor,1}$ = 0.5 mm, $\bar{t}_{cr,a}$ = 0.30. (b) Bonded trabecular bone, $t_{cor,2}$ = 0.4 mm, $\bar{t}_{cr,b}$ = 0.64. (c) Bonded trabecular bone, $t_{cor,3}$ = 0.2 mm, $\bar{t}_{cr,c}$ = 0.74. (d) Unbonded trabecular bone, $t_{cor,3}$ = 0.2 mm, $\bar{t}_{cr,d}$ = 0.16.

The stress field characteristics are shown in Figure 4. The distribution of von Mises stress on the cortical shell is presented analogously to the previous picture. It is clearly seen that bonded and unbonded cortical walls exhibit completely different resistance.

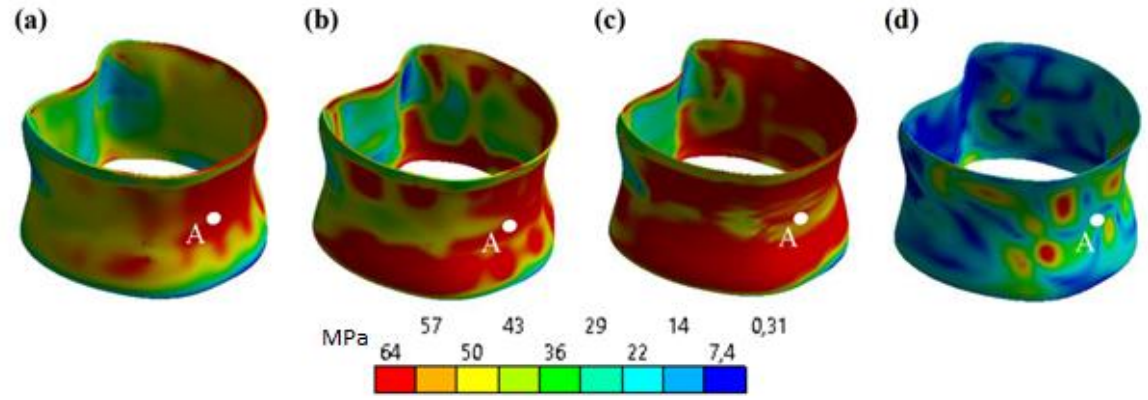

Figure 4: The von Mises stress σ (MPa) distribution on the cortical bone at the first bifurcation point. (a) Bonded trabecular bone, $t_{cor,1}$ = 0.5 mm, $\bar{t}_{cr,a}$ = 0.30. (b) Bonded trabecular bone, $t_{cor,2}$ = 0.4 mm, $\bar{t}_{cr,b}$ = 0.64. (c) Bonded trabecular bone, $t_{cor,3}$ = 0.2 mm, $\bar{t}_{cr,c}$ = 0.74. (d) Unbonded trabecular bone, $t_{cor,3}$ = 0.2 mm, $\bar{t}_{cr,d}$ = 0.16.

The bonded case (Fig. 4 a, b, c) shows high volumes of stress, indicating higher resistance, while the unbonded case (Fig. 4 d) is characterised by substantially lower stress values, indicating high deformations due to small loads.

4.Discussion

The discussion on the failure mechanism is based on the obtained results and aims to discover the role of buckling in the load-bearing capacity of the L1 vertebral body. Here, the lower

bound of the safety margin is identified as a parameter that reflects fracture risk, which includes not only the classical compressive strength criterion but also the deformation criterion that reflects large deformations leading to local instabilities.

The essential properties of the compressed body are characterised by the force-displacement relationship. The numerical results are shown in Figure 5.

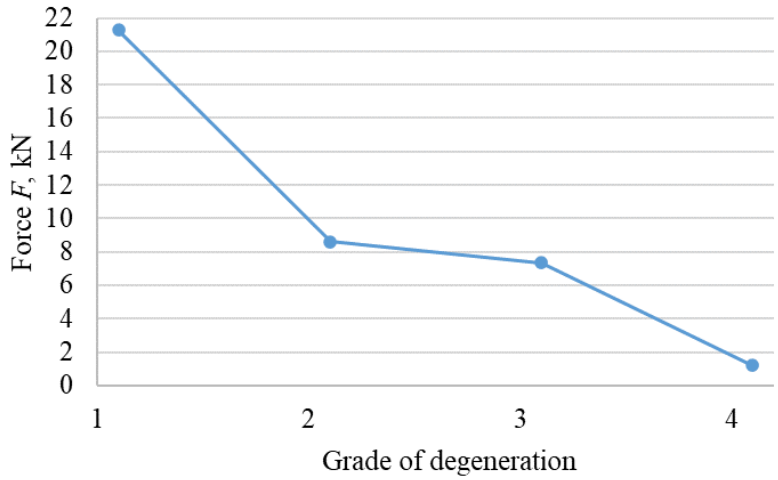

Fig. 5. Comparison of maximum compression load versus age-related degeneration at time t_{max}.

Here, the change in compressive load is presented as a function of the degree of vertebral degeneration at $u_{z,max}$ and $\omega_{z,max}$.

When the mass of the trabecular bone and the thickness of the cortex decrease, the value of the compressive load decreases significantly. As the cortical layer decreases from 0.5 mm (Grade 1) to 0.4 mm of the osteoporotic vertebra (Grade 2), the maximum axial force decreases almost two and a half times, from $F_1\,(t_{max}) = 21.3$ kN to $F_2\,(t_{max}) = 8.6$ kN.

A further reduction in the cortical bone thickness of the osteoporotic vertebra to 0.2 mm (Grade 3) slightly affects the axial force compared to Grade 2, and its value is $F_3\,(t_{max}) = 7.3$ kN. However, if the osteoporotic vertebra has gaps between the cortex and the trabecular bone (Grade 4), the axial force is reduced six-fold to $F_4\,(t_{max}) = 1.21$ kN compared to the same osteoporotic vertebra without a trabecular bone defect (Grade 3).

The variation of von Mises stress at a selected point A is shown in Figure 6. Here, the variation of von Mises stress is plotted against relative time $\bar{t} = t / t_{max}$. The relative time ranges between the 0 and 1 interval ($0 < \bar{t} < 1$) and illustrates the behaviour of the structure during the loading state. The time scale also reflects displacement ($0 < u(t) \leq u_{z,max}\,(t_{max})$). The location of point A is chosen in advance to illustrate the typical situation of cortical shell

behaviour. To understand the safety margin, a von Mises stress contour plot is shown in Figure 4 in the frontal view of the cortical bone.

The first three curves, denoted as Curve a, Curve b, Curve c, illustrate the variation of specified quantities corresponding to three values of cortex thickness $t_{cor,1}$ = 0.5 mm, $t_{cor,2}$ = 0.4 mm, $t_{cor,3}$ = 0.2 mm, in the case of perfect bonding. The fourth curve, Curve d, illustrates the time variation of these quantities for the case of degenerated bond considering displacement at the cortex thickness of $t_{cor,3}$ = 0.2 mm (Fig. 5). The presence of critical loads $F_{cr,a}$, $F_{cr,b}$, $F_{cr,c}$, $F_{cr,d}$ was confirmed by considering the variation of horizontal displacement $u_x(t)$ at point A (Fig. 6). It was found that the obtained critical loads illustrate different behaviour in the presence of a perfect bond. The first bifurcation point is denoted by thin lines indicating critical displacement on a horizontal axis and critical load on a vertical axis.

Both unbonded and bonded structures illustrate different post-buckling behaviour. For the bonded case, bifurcation points stand for total stability load with unstable post-buckling behaviour. For the unbonded case, bifurcation points indicate local instability and secondary stable equilibrium.

The variation between force and displacement in the horizontal direction $u_x(t)$ at point A explains post-buckling behaviour after bifurcation. Descending of horizontal displacement (Fig. 6) indicates unstable motion after buckling. Global post-buckling instability defined by an unlimited drop of displacement corresponds to the case of a bonded shell-solid connection (Curves a, b, c). For the case of osteoporotic bonding, the secondary stability past is indicated. It is characterised by secondary branches of ascending loading (Curve d) (Fig. 6).

Based on the numerical results (Curve a) obtained for healthy vertebrae with a shell thickness of 0.5 mm (Grade 1), it was found that the load-bearing capacity of vertebrae is characterised by the strength criterion. The time histories of the von Mises stress σ (Fig. 7) show that the strength criterion $\sigma_y \approx 64$ MPa for the case under compression with torsion is satisfied at time instant $\bar{t}_{cr,a}$ = 0.30. Moreover, the local displacement $u_{x,a}$ ($\bar{t}_{cr,a}$) = 0.08 mm (Fig. 6) is relatively small, while the load at time instant $\bar{t}_{cr,a}$ may be considered as the limit load $F_{cr,a}$ = 12.7 kN. The distribution of von Mises stress (Fig. 4) confirms this statement clearly.

The behaviour of osteoporotic bonded vertebrae with a shell thickness between 0.4 mm and 0.2 mm under compression with torsion (Curves b, c) can be characterised in the same way. The time histories of the von Mises stress σ (Fig. 7) show that the strength criterion $\sigma_y \approx 64$ MPa for Grade 2 is reached at time instant $\bar{t}_{cr,b}$ = 0.64. However, the local displacement $u_{x,b}$ ($\bar{t}_{cr,b}$) = 0.21 mm (Fig. 6) is considerably higher, and the lower limit of the

load limit has been halved to $F_{cr,b}$ = 6.39 kN. The distribution of von Mises stress is shown in Figure 4.

When reducing the shell thickness to 0.2 mm (Grade 3), the time histories of the von Mises stress σ (Fig. 7) show that the strength criterion $\sigma_y \approx 64$ MPa is satisfied at time instant $\bar{t}_{cr,c}$ = 0.74. However, the local displacement $u_{x,c}$ ($\bar{t}_{cr,c}$) = 0.32 mm (Fig. 6) is insignificantly smaller, and the load at time instant $\bar{t}_{cr,c}$ may be considered as the limit load $F_{cr,c}$ = 6.12 kN. The distribution of von Mises stress (Fig. 4) clearly confirms this statement.

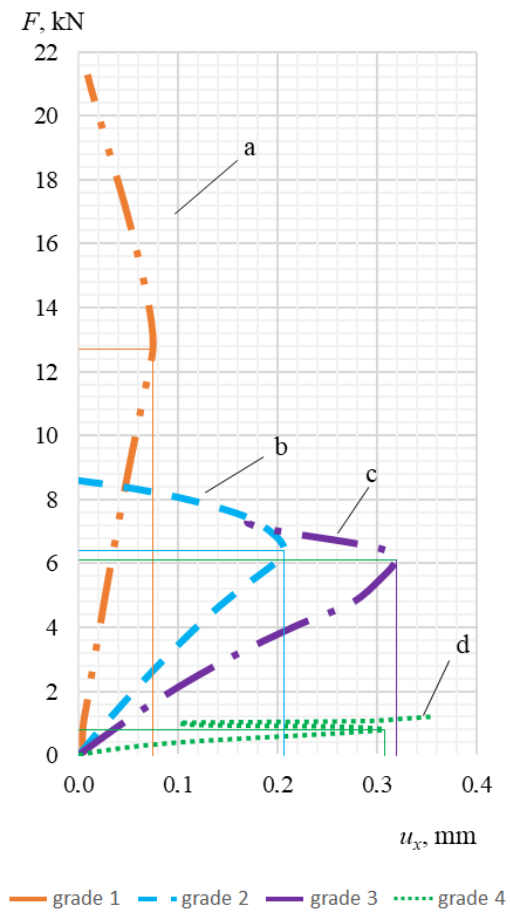

Figure 6: Graph of the horizontal displacement $u_x(t)$ at point A as a dependency of the load.

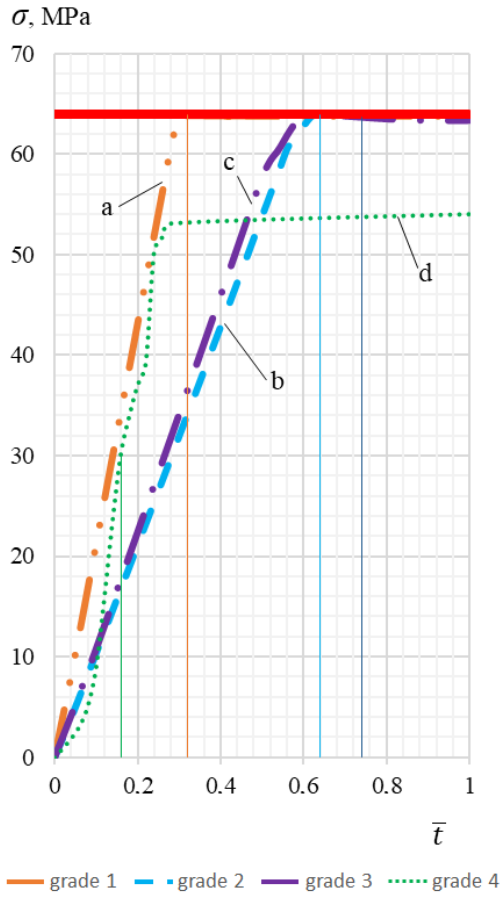

Figure 7: Graph of the von Mises stress change at point A in time.

According to statistical data, it is safe to assume that a decrease in trabecular bone density most often occurs near the front vertebral wall, which causes a gap to form between the trabecular and cortical bones. With the appearance of a gap between cortical and trabecular bones, the behaviour of the vertebral body defined by Curve d is different. The variation of displacement (Fig. 6) clearly shows the presence of a critical point at time instant $\bar{t}_{cr,d}$ = 0.16 (Grade 4). Consequently, load-bearing capacity is predefined by the critical buckling load

$F_{cr,d}$ = 0.80 kN (Fig. 6). This load is characterised by the elastic state, σ ($\bar{t}_{cr,d}$) = 30 MPa < 64 MPa (Fig. 7).

Even lower values may be required to limit transverse displacement. With degeneration of the trabecular bone, cortical bone thickness does not have as significant an impact on the vertebra's load capacity as the formation of voids near the cortical bone. When the shell thickness was reduced to 0.2 mm (Grade 4), a displacement $u_{x,d}$ ($\bar{t}_{cr,d}$) = 0.31 mm, which was 150% larger than the shell thickness, appeared. Therefore, when compressing a degenerated vertebra, the time history of the transverse displacement at point A (Fig. 6) exhibits an unlimited character, illustrating unstable deformation behaviour.

Mentioned results fall within the range of 1000–6000 N, established by Lohmüller et al. [20], who measured the compressive failure load in osteoporotic elderly patients, with an average age of 82 years, as well as with numerical results obtained by McDonald et al. [25] during the modelling and computer FE analysis of osteoporotic vertebrae.

The performed numerical stability analyses of lumbar vertebrae have revealed that the presence of local degradation between cortical and trabecular bones may lead to catastrophic consequences in the mechanical behaviour of lumbar vertebrae. The disappearance of a bond leads to local instability in the form of buckling.

The failure mechanism shown in Figures 6 and 7 was determined for specific bone density values that are assumed to be homogeneous within each subvolume. For wider range of results, it would be of great interest to observe how the failure mechanism changes at different density values. Histomorphometric data used to calculate density may only be available for patients with osteoporosis who have undergone vertebroplasty [7]. The availability of histomorphometric data for other patients is very limited [7]. An alternative approach that could be taken in this case is to use CT data for density estimation. This approach was followed, for example, by Petrushak et al. [31] in analysing the mechanism of human femur fractures. The computational model presented in this study analysis was used for the failure mechanism only under static conditions. In further studies for the reliability of the results, fatigue analysis would be desirable [34].

Gerontologists determine the degree of osteoporotic degeneration based on the density loss of the trabecular bone. The criterion for the risk of vertebral fractures is a decrease in the height of the osteoporotic vertebra. The results of the numerical modelling revealed the instability of the deformity resulting from osteoporotic bone degeneration. In addition to the vertical decrease of the vertebra dimensions, another important criterion is the decrease of the horizontal dimensions.

It is important to note that local deformation criteria, including buckling, should be used to determine fracture risk. Changes in cortical bone thickness and areas of major disruption between cortical and trabecular bone must be evaluated, not just mean trabecular bone density.

The presented results cannot yet be directly applied in medical practice, since the created models describe segregate, essentially hypothetical cases of bone tissue pathology. Any study involving computer modelling is not without various degrees of limitations. Our presented work is no exception. Firstly, the model used in this study was reconstructed based on the lumbar spine of a healthy patient. Secondly, the study is limited to a single sample. Thirdly, the loading conditions used in the current study do not fully reflect the real physiological situation. Fourthly, the current problem may be associated with many research areas, such as cell biology, molecular biology, immunohistochemistry and biomechanics. In this study, we analysed the impact of osteoporosis on loss of load-bearing capacity solely from the perspective of biomechanics. Therefore, additional research is needed in the future.

Data Availability

The data presented in this study are available on request from the corresponding author.

References

[1] AYTURK U., PUTTLITZ C., *Parametric convergence sensitivity and validation of a finite element model of the human lumbar spine*, Comput Methods Biomech Biomed Eng., 2011, 14, 695–705

[2] BLANCHARD R., MORIN C., MALANDRINO A., et al, *Patient-specific fracture risk assessment of vertebrae: A multiscale approach coupling X-ray physics and continuum micromechanics*, Int. J. Numer. Method. Biomed. Eng., 2016, 32, 1–36

[3] CHABAROVA O., ALEKNA V., KAČIANAUSKAS R., ARDATOV O., *Finite element investigation osteoporotic lumbar L1 vertebra buckling in a presence of torsional load*, Mechanics, 2017, 23, 326–333

[4] CHABAROVA O., KAČIANAUSKAS R., ALEKNA V., *Buckling of osteoporotic lumbar: finite element analysis : research article*, Research in medical & engineering sciences, 2019, 8(2), DOI: 10.31031/RMES.2019.08.000683.

[5] CHABAROVA O., *Numerical investgation of the effect of bone tissue pathology on human spine stability*, Dissertation, Vilnius Gediminas Technical University, 2020.

[6] CHOTAI S., GUPTA R., PENNINGS J.S., et al, *Frailty and Sarcopenia: Impact on Outcomes Following Elective Degenerative Lumbar Spine Surgery*, Spine (Phila Pa 1976), 2022, 47, 1410–1417, DOI: https://doi.org/10.1097/BRS.0000000000004384

[7] DIAMOND T. H., CLARK W. A., AND KUMAR S. V., *Histomorphometric analysis of fracture healing cascade in acute osteoporotic vertebral body fractures*. Bone, 2007, 40, 775–780

[8] DU H.G., LIAO S.H., JIANG Z., et al, *Biomechanical analysis of press-extension technique on degenerative lumbar with disc herniation and staggered facet joint*, Saudi Pharm. J., 2016, 24, 305–311

[9] FINLEY S.M., BRODKE D.S., SPINA N.T., et al, *FEBio finite element models of the human lumbar spine*, Comput. Methods. Biomech. Biomed. Engin., 2018, 21, 444–452, DOI: https://doi.org/10.1080/10255842.2018.1478967

[10] GARGES K.J., NOURBAKHSH A., MORRIS R., et al, *A Comparison of the Torsional Stiffness of the Lumbar Spine in Flexion and Extension*, J. Manipulative. Physiol. Ther., 2008, 31, 563–569

[11] GHADIRI M., *Fracture Mechanics Analysis of Fourth Lumbar Vertebra in Method of Finite Element Analysis*, Int. J. Adv. Biol. Biom. Res., 2014, 2, 2217–2224

[12] HAMILTON E.J., GHASEM-ZADEH A., GIANATTI E., et al, *Structural Decay of Bone Microarchitecture in Men with Prostate Cancer Treated with Androgen Deprivation Therapy*, J. Clin. Endocrinol. Metab., 2010, 95, E456–E463

[13] HUANG K., ZHANG J., *Three-dimensional lumbar spine generation using variational autoencoder*, Med. Eng. Phys., 2023, 120, 104046, DOI: https://doi.org/10.1016/J.MEDENGPHY.2023.104046

[14] JIANG Y., LIN D., GUO X., et al, *Vertebral fractures are likely to occur in lumbar vertebra in patients with osteoporosis and even in osteopenia*, Jt. Bone Spine., 2018, 77, 1627–1627, DOI: https://doi.org/10.1136/annrheumdis-2018-eular.5051

[15] JOHANSEN J.G., NORK M., GRAND F., *Torsional instability of the lumbar spine*, Riv. Neuroradiol., 1999, 12, 193–195

[16] JONES A.C., WILCOX R.K., *Finite element analysis of the spine: Towards a framework of verification, validation and sensitivity analysis*, Med. Eng. Phys., 2008, 30, 1287–1304

[17] KIM Y.H., WU M., KIM K., *Stress Analysis of Osteoporotic Lumbar Vertebra Using Finite Element Model with Microscaled Beam-Shell Trabecular-Cortical Structure*, J. Appl. Math., 2013, 1–6

[18] KINZL M., SCHWIEDRZIK J., ZYSSET P.K., PAHR D.H., *An experimentally validated finite element method for augmented vertebral bodies*, Clin. Biomech., 2013, 28, 15–22

[19] LAN C., KUO C., CHEN C., HU H., *Finite element analysis of biomechanical behavior of whole thoraco-lumbar spine with ligamentous effect*, CJM, 2013, 26–41

[20] LOCHMÜLLER E. M., ECKSTEIN F., KAISER D., ZELLER J. B., LANDGRAF J., PUTZ, R., AND STELDINGER R., *Prediction of vertebral failure loads from spinal and femoral dual-energy X-ray absorptiometry, and calcaneal ultrasound: an in situ analysis with intact soft tissues*, Bone, 1998, 23, 417–424

[21] LOUGHENBURY P.R., TSIRIKOS A.I., GUMMERSON N.W., *Spinal biomechanics - biomechanical considerations of spinal stability in the context of spinal injury*, Orthop Trauma, 2016, 30, 369–377

[22] MADENCI E., GUVEN I., *Fundamentals of Discretization. In: The Finite Element Method and Applications in Engineering Using ANSYS*, Springer US, 2015, 35–74
[23] MAKNICKAS A., ALEKNA V., ARDATOV O., et al, *FEM-based compression fracture risk assessment in osteoporotic lumbar vertebra L1*, Appl. Sci.-Basel, 2019, 9, DOI: https://doi.org/10.3390/APP9153013
[24] MAZLAN M.H., TODO M., TAKANO H., YONEZAWA I., *Finite Element Analysis of Osteoporotic Vertebrae with First Lumbar (L1) Vertebral Compression Fracture*, IJAPM, 2014, 4, 267–274
[25] MCDONALD K.; LITTLE J.; PEARCY, M.; ADAM, C., *Development of a Multi-Scale Finite Element Model of the Osteoporotic Lumbar Vertebral Body for the Investigation of Apparent Level Vertebra Mechanics and Micro-Level Trabecular Mechanics*. K. Med. Eng. Phys., 2010, 32, 653–661
[26] MOLINARI L., FALCINELLI C., *On the human vertebra computational modeling: a literature review*, Meccanica, 2022, 57, DOI https://doi.org/10.1007/s11012-021-01452-x
[27] MOLINARI L., FALCINELLI C., GIZZI A., DI MARTINO A., *Effect of pedicle screw angles on the fracture risk of the human vertebra: A patient-specific computational model*, J. Mech. Behav. Biomed. Mater.,2021, 116, 104359, DOI: https://doi.org/10.1016/J.JMBBM.2021.104359
[28] MONTEIRO N.M.B., DA SILVA M.P.T., FOLGADO J.O.M.G., MELANCIA J.P.L., *Structural analysis of the intervertebral discs adjacent to an interbody fusion using multibody dynamics and finite element cosimulation*, Multibody Syst. Dyn., 2011, 25, 245–270
[29] OKAMOTO Y., MURAKAMI H., DEMURA S., et al, *The effect of kyphotic deformity because of vertebral fracture: a finite element analysis of a 10° and 20° wedge-shaped vertebral fracture model*, The Spine Journal, 2015, 15, 713–720
[30] POLIKEIT A., NOLTE L.P., FERGUSON S.J., *Simulated influence of osteoporosis and disc degeneration on the load transfer in a lumbar functional spinal unit*, J. Biomech., 2004, 37, 1061–1069
[31] PIETRUSZCZAK S., INGLIS D., PANDE G. N., *A fabric-dependent criterion for bone*, J. Biomechanics, 1999, 32, 1071–1079
[32] PROVATIDIS C., VOSSOU C., KOUKOULIS I., et al, *A pilot finite element study of an osteoporotic L1-vertebra compared to one with normal T-score*, Comput. Methods. Biomech. Biomed. Engin., 2010, 13.185–195, DOI https://doi.org/10.1080/10255840903099703
[33] SU X., SHEN H., SHI W., et al, *Dynamic characteristics of osteoporotic lumbar spine under vertical vibration after cement augmentation*, Am. J. Transl. Res., 2017, 9, 4036–4045
[34] TAYLOR D., *Scaling effects in the fatigue strength of bones from different animals*, J. Theor. Biology, 2000, 206, 299–306.
[35] YANG L., DEMPSEY M., BRENNAN A., et al (2023) *Ireland DXA-FRAX may differ significantly and substantially to Web-FRAX*, Arch. Osteoporos., 2023, 18, 43, DPI https://doi.org/10.1007/S11657-023-01232-Y

[36] YANG S., XIA H., CONG M., et al, *Unilateral pedicle screw fixation of lumber spine: A safe internal fixation method*, Heliyon, 2022, 8, e11621, DOI https://doi.org/10.1016/j.heliyon.2022.e11621
[37] ZAHAF S., HABIB H., MANSOURI B., et al, *The Effect of the Eccentric Loading on the Components of the Spine*, Global Journals Inc., 2016, 16, 2249–4596
[38] ZEBAZE R.M., GHASEM-ZADEH A., BOHTE A., et al, *Intracortical remodelling and porosity in the distal radius and post-mortem femurs of women: a cross-sectional study*, The Lancet, 2010, 375, 1729–1736
[39] ZHU R., NIU W.X., ZENG Z.L., et al, *The effects of muscle weakness on degenerative spondylolisthesis: A finite element study*, Clin. Biomech., 2017, 41, 34–38
[40] *3D Slicer image computing platform*, Available online: https://www.slicer.org/, Accessed on 8 January 2023
[41] *Ansys. Engineering Simulation Software*, Available online: https://www.ansys.com/, Accessed on 8 January 2023
[42] *MeshLab*, Available online: https://www.meshlab.net/, Accessed on 8 January 2023
[43] *SOLIDWORKS. 3D CAD Design Software & PDM Systems*, Available online: https://www.solidworks.com/, Accessed on 8 January 2023